ELSEVIER

Biophysical Chemistry 122 (2006) 16–26

Biophysical Chemistry

http://www.elsevier.com/locate/biophyschem

Analysis of absorption spectra of purple bacterial reaction centers in the near infrared region by higher order derivative spectroscopy

I.K. Mikhailyuk [a], P.P. Knox [b], V.Z. Paschenko [b], A.P. Razjivin [a], H. Lokstein [c,*]

[a] *A.N. Belozerski Institute of Physico-Chemical Biology, Biology Faculty of the M.V. Lomonosov Moscow State University, 119992, Moscow, Russia*
[b] *Department of Biophysics, Biology Faculty of the M.V. Lomonosov Moscow State University, 119992, Moscow, Russia*
[c] *Institut für Biochemie und Biologie/Pflanzenphysiologie, Universität Potsdam, Karl-Liebknecht-Str. 24-25, Haus 20, D-14476 Golm, Germany*

Received 18 October 2005; received in revised form 9 February 2006; accepted 9 February 2006
Available online 28 February 2006

Abstract

Reaction centers (RCs) of purple bacteria are uniquely suited objects to study the mechanisms of the photosynthetic conversion of light energy into chemical energy. A recently introduced method of higher order derivative spectroscopy [I.K. Mikhailyuk, H. Lokstein, A.P. Razjivin, A method of spectral subband decomposition by simultaneous fitting the initial spectrum and a set of its derivatives, J. Biochem. Biophys. Methods 63 (2005) 10–23] was used to analyze the NIR absorption spectra of RC preparations from *Rhodobacter* (*R.*) *sphaeroides* strain 2R and *Blastochloris* (*B.*) *viridis* strain KH, containing bacteriochlorophyll (BChl) *a* and *b*, respectively. Q_y bands of individual RC porphyrin components (BChls and bacteriopheophytins, BPheo) were identified.

The results indicate that the upper exciton level P_{y+} of the photo-active BChl dimer in RCs of *R. sphaeroides* has an absorption maximum of 810 nm. The blue shift of a complex integral band at approximately 800 nm upon oxidation of the RC is caused primarily by bleaching of P_{y+}, rather than by an electrochromic shift of the absorption band(s) of the monomeric BChls. Likewise, the disappearance of a band peaking at 842 nm upon oxidation of RCs from *B. viridis* indicates that this band has to be assigned to P_{y+}. A blue shift of an absorption band at approximately 830 nm upon oxidation of RCs of *B. viridis* is also essentially caused by the disappearance of P_{y+}, rather than by an electrochromic shift of the absorption bands of monomeric BChls. Absorption maxima of the monomeric BChls, B_B and B_A are at 802 and 797 nm, respectively, in RCs of *R. sphaeroides* at room temperature. BPheo co-factors H_B and H_A peak at 748 and 758 nm, respectively, at room temperature. For *B. viridis* RCs the spectral positions of H_B and H_A were found to be 796 and 816 nm, respectively, at room temperature.

Keywords: Absorption spectra; Bacterial reaction center; Derivative spectroscopy; Higher-order derivatives; *Rhodobacter sphaeroides*; *Blastochloris viridis*

1. Introduction

Purple bacterial reaction centers (RCs) are uniquely suitable objects to study the mechanisms of the highly effective photosynthetic conversion of light energy into chemical energy. Since the pioneering work of Deisenhofer et al. [1] highly resolved X-ray crystal structural analyses have become available for RCs of several purple bacterial species, e.g. Refs. [2–4], facilitating the establishment of structure–function relationships. RCs are membrane-integral pigment–protein complexes, binding 4 bacteriochlorophyll (BChl) molecules, two bacteriopheophytins (BPheo, also denoted as H), two quinones (Q) and a non-heme iron co-factor [1–4]. Two strongly excitonically coupled BChl molecules form the photoactive dimer of the primary electron donor (P). Monomeric BChls (in the following denoted as B) and BPheos are organized in two nearly symmetric (with respect to the C_2 axis running through P and the non-heme iron) branches in the RC —indexed A and B. Under normal conditions, primary charge separation and further electron transfer (up to Q_A) occur only in

Abbreviations: BChl, bacteriochlorophyll; B, monomeric accessory BChls; BPheo or H, bacteriopheophytin; Q_A, primary quinone acceptor; EET, excitation energy transfer; FWHM, full width at half maximum; LDAO, lauryldimethylamine-oxide; NIR, near infrared; P, primary electron donor; P_{y+} and P_{y-}, symmetric and antisymmetric components of the Q_y transition of P; RC, reaction center; RT, room temperature; *B.*, *Blastochloris*; *R.*, *Rhodobacter*.

* Corresponding author. Tel.: +49 331 977 2648; fax: +49 331 977 2512.
E-mail address: lokstein@uni-potsdam.de (H. Lokstein).

0301-4622/$ - see front matter © 2006 Elsevier B.V. All rights reserved.
doi:10.1016/j.bpc.2006.02.002

the A-branch. The sequence and kinetics of photoexcitation and electron transfer steps in the purple bacterial RC at room temperature (RT) can be summarized as follows e.g. Refs. [5–7], see also a recent review [8]:

$$h\nu \xrightarrow{\sim 3ps} {}^{*}P_{B_A}H_AQ_A \xrightarrow{\sim 1ps} P^{+}B_A^{-}H_AQ_A \xrightarrow{\sim 200ps} P^{+}B_AH_A^{-}Q_A \rightarrow P^{+}B_AH_AQ_A^{-}$$

The spectral positions of the lowest-energy (Q_y) absorption bands of the pigments in RCs in the near infrared (NIR) region have gained long-standing experimental and theoretical interest, in particular due to the fact that the Q_y absorption bands of these components are red shifted by more than 100 nm in comparison to isolated pigments in organic solution. Different explanations have been proposed, i.e., an influence of the electric field of charged amino acid residues of the apoprotein [9], and/or excitonic interactions between the pigments [10,11].

Elucidating the origin of this shift has pivotal importance for understanding excitation energy transfer (EET) and charge separation in the RC [12,13]. These processes, the initial stages of which occur on the femtosecond timescale, require a precise energetic match of the individual pigments electronic transitions. Thus, elucidation of the nature of interaction of the bacteriochlorin co-factors and of the mechanisms of electron density redistribution between the components with subsequent formation of the charge transfer complexes is the object of intensive ongoing study. Absorption spectra of bacterial RCs are very complex due to the strong overlap between the electronic transitions of the individual co-factors [14].

Transitions observed at 540, 600, 790, 830 and 960 nm in RCs of *Blastochloris* (*B.*) *viridis*—a BChl *b* containing purple bacterium—at RT have been assigned previously to specific co-factors [2,15–18]: a band located at 540 nm at 300 K is a superposition of the Q_x transitions of both BPheos, a band near 600 nm is due to overlapping Q_x bands of all BChls in the RC. The Q_y peak of the BPheos at 790 nm (at RT) can be resolved at low temperature into two subbands (at 790 and 810 nm) assigned to H_B and H_A, respectively [18]. In the spectral region around 830 nm, contributions of all BChl RC components are found [15–20]. Consequently, number, spectral position, and width of the pigment absorption subbands in the NIR region are of fundamental importance for a detailed interpretation of the mechanism(s) of RC function. Moreover, results obtained by theoretical calculations of the spectral characteristics of the absorption bands depend critically on the initial model parameters [21] — for which precise values were not available up to now. It is generally assumed that the two BChls forming the primary electron donor P are coupled by strong excitonic interaction. As a consequence of this interaction two excitonic bands appear, corresponding to the symmetric (P_{y+}) and antisymmetric (P_{y-}) components of the Q_y transition. Of particular importance to understand RC function is the knowledge of the precise spectral position of its upper excitonic level, P_{y+}.

The P_{y-} band peaks at approximately 960 nm (at 300 K) in *B. viridis* RCs. Nevertheless, the exact spectral position of the P_{y+} band cannot be easily deduced due to the strong overlap of B and P_{y+} absorption bands—rendering it very difficult to deconvolute respective spectra.

Consequently, deduced P_{y+} positions for RCs of *B. viridis* vary considerably: a theoretical analysis of absorption and CD spectra of RCs suggested a value of 811 nm for the P_{y+} maximum [11]. LD studies indicated that P_{y+} is located at 850 nm [16]. Based on dichroic transient absorption spectroscopy, P_{y+} was determined to peak at 855 nm [21].

The absorption spectrum of RCs of the BChl *a* containing purple bacterium *Rhodobacter* (*R.*) *sphaeroides* is characterized by transitions at 540, 600, 760, 802 and 865 nm at RT [2,14,15]. Bands at 540 and 600 nm are due to the overlapping Q_x transitions of the BPheos and of all RC BChls, respectively. At low temperature the Q_x band of the BPheos resolves into two transitions at 546 (H_A) and 533 nm (H_B) [22].

The band at 802 nm is thought to be mainly due to Q_y transitions of the two monomeric BChls (at 300 K). Attempts to determine individual positions of B_A and B_B at RT have been made by pigment exchange [23,24], but have to be further substantiated with native RCs. However, at 20 K these species absorb at 802 and 810 nm, respectively [22]. In addition to B_A and B_B, contributions of P_{y+} and P_{y-} to the absorption band at about 800 nm have to be presumed.

The lower excitonic level of the special pair, P_{y-}, is obviously associated with an absorption band 865 at RT. Due to strongly overlapping Q_y transitions of B_A, B_B and P_{y+} an exact position of the latter, in particular at RT, has not been determined so far. P_{y+} absorption in RCs of *R. sphaeroides* has been found to vary from 805 to 825 nm in previous studies [12,23,25–28]. Based on linear dichroism spectra it was concluded that at the P_{y+} maximum is at 814 or 815 nm at 77 K [25,26]. Photochemical hole-burning experiments at 4.2 K facilitated identification of the P_{y+} maximum at 811 nm [27]. Photon echo studies at 77 K suggested a P_{y+} maximum position at 813 nm [28]. Absorption spectra of modified RCs indicated a localization of P_{y+} between 805 and 810 nm at 8 K [23]. According to Ref. [12], the P_{y+} maximum is located at 825 nm at 298 K.

To identify individual Q_y absorption bands of RC components and their band parameters, a method of higher-order derivative spectroscopy as developed by us [29] is expected to be advantageous. In the present work this technique was used to analyze the NIR absorption spectra of RC preparations from *R. sphaeroides* strain 2R and *B. viridis* strain KH, containing BChl *a* and *b*, respectively.

2. Materials and methods

Purple photosynthetic bacteria of the wild-type strains *R. sphaeroides* 2R and *B. viridis* KH were obtained from the Microbiology Department, Faculty of Biology, M.V. Lomonosov Moscow State University. RCs of *R. sphaeroides* strain 2R were isolated from chromatophores by solubilization with 0.5% (w/v) lauryldimethylamine-oxide (LDAO) in 10 mM sodium phosphate buffer (pH 7.0) at 4 °C for 30 min. The isolation procedure is described in detail in Ref. [30]. Isolated RCs of *R. sphaeroides* were suspended in 10 mM sodium phosphate buffer

(pH 7.0) containing 0.05% (w/v) LDAO. Subsequently, LDAO was replaced by 0.1% (w/v) sodium cholate via dialysis. These preparations proved to be more stable during long-term storage. For the experiments, RCs in 10 mM sodium phosphate buffer (pH 8.1), containing 0.1% (w/v) sodium cholate were used. Absorption spectra of RC preparations containing LDAO did not vary from preparations containing sodium cholate.

RCs of *B. viridis* strain KH were isolated by hydroxylapatite column chromatography following solubilization of chromatophores in 1% (w/v) LDAO solution. The isolation procedure is described in detail in Ref. [30]. Isolated RCs were suspended in 10 mM sodium phosphate buffer (pH 7.0) containing 0.05 % (w/v) LDAO.

Absorption spectra of the samples were measured in a 1 cm pathlength cuvette using a Shimadzu 1601 spectrophotometer. Maximum absorption in the NIR region did not exceed 1. UV/VIS/NIR absorption spectra of RC preparations of *R. sphaeroides* strain 2R and *B. viridis* strain KH are shown in Fig. 1. The 280 to 800 nm absorbance ratio is taken as a measure of purity of the *R. sphaeroides* RC preparation, usually being 1.3–1.5. This ratio indicates that RC preparations containing sodium cholate did not vary in BChl content from RC preparations in LDAO. For *B. viridis* RC preparations the 280 to 830 nm absorbance ratio was 2.3–2.5 which is usual. Moreover, the spectra in Fig. 1 indicate that no carotenoids were lost during preparation of the RCs.

For chemical oxidation of the photoactive pigments potassium ferricyanide (1 mM for *R. sphaeroides* and 5 mM for *B. viridis*) was used. For low-temperature measurements glycerol was added to 70% (v/v).

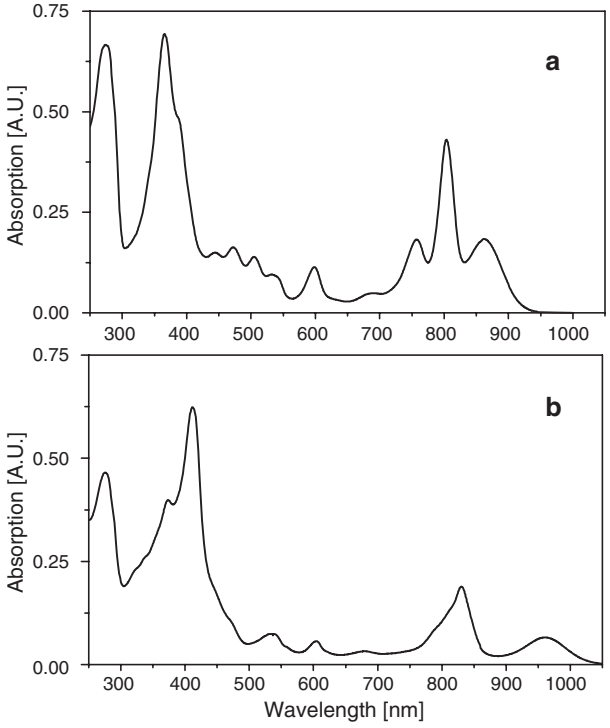

Fig. 1. Room temperature UV/VIS/NIR absorption spectra of RC preparations from the BChl *a* containing purple bacterium *R. sphaeroides* strain 2R (a) and from the BChl *b* containing purple bacterium *B. viridis* strain KH (b).

The decomposition of the initial spectrum into standard (Gaussian) bands and the collection of undistorted derivatives was done using the programs "Derint" and "Deriv" employing a previously developed procedure. The method is described in detail in Ref. [29]. Basic assumptions were as follows: since there is no simple analytical description of the form of an absorption band [31], for the approximation standard functions such as Gaussians, Lorentzians or their combination (Voigtians) were used. In the current paper, to approximate one experimental band 2–4 Gaussian subbands are used. Usually, the narrowest band(s) provide(s) the essential contribution(s), the maximum of which generally coincides with the maximum of experimental band. Broader bands serve to improve the approximation of the wings of experimental bands.

To obtain higher derivatives it is necessary to smooth the original experimental spectra (i.e., filter out high frequencies). The selection procedure of an optimal filter as proposed by us [29] is the following: from analysis of the experimental spectrum and its second derivative obtained without (or with minimal necessary) smoothing, the width (full width at half maximum, FWHM) of the narrowest band of the spectrum is estimated. Subsequently, a model spectrum (Gaussian) of the same FWHM is generated. Random (white) noise of the same amplitude as in the experimental spectrum is added. Derivatives up to some maximum order are calculated analytically for the Gaussian model band without noise. Thereafter the Gaussian model band *with* added noise undergoes smoothing (filtering) followed by numerical differentiation. Results are compared and the order of the derivative for which the curves, obtained analytically and with the aid of smoothing/differentiation differ, e.g., no more than 10% is determined. The same procedure of smoothing/differentiation is applied to the experimental spectrum. It is assumed that the derivatives from the first to the sixth order will also differ from the unknown true derivative by no more than 10%. These derivatives are called undistorted derivatives, and the filter (smoothing procedure) used is called optimum filter. The (initial) experimental absorption spectrum and the entire set of undistorted derivatives are used for the decomposition into Gaussian bands. Narrow bands are selected first, giving the major contributions to higher derivatives. Broad bands determine the form of the initial spectrum and of lower derivatives. In the program package filtering out of high frequencies is accomplished by Fourier transform. Errors of the quantitative band parameters (maximum, amplitude and FWHM) are obtained by expert estimation. Usually parameters of narrow bands are determined with an accuracy on the order of 5–10%, those of broad bands with an accuracy of 15–20%.

3. Results and discussion

3.1. Analysis of the absorption spectra of RCs from B. viridis

RT absorption spectra on the NIR region of native (reduced) and chemically oxidized RCs of the BChl *b* containing purple bacterium *B. viridis* strain KH are presented in Figs. 2 and 3, respectively. These spectra are normalized at 830 nm. Experimental absorption spectra were decomposed into Gaussian

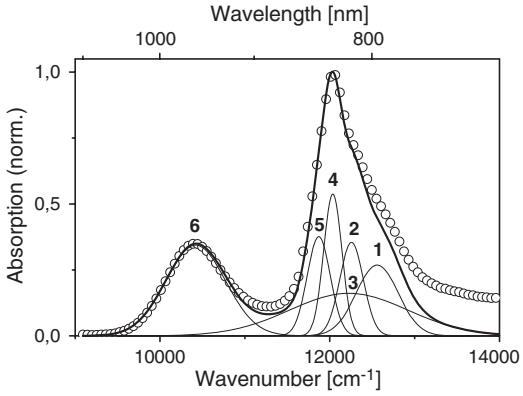

Fig. 2. Room temperature Q_y absorption spectrum of reduced RCs from the BChl *b* containing purple bacterium *B. viridis* strain KH (circles). Gaussian bands into which the experimental spectrum was decomposed are shown as thin curves. The thick curve represents the envelope of the Gaussian subbands.

bands (thin curves), their envelope (thick curve) is shown, too. Each model band is characterized by three parameters—absorption maximum, normalized relative amplitude and FWHM. Derivatives (considered to be undistorted, vide supra) of the spectra up to the 6th order were used. The spectrum of reduced RCs can be decomposed into 6 Gaussian bands (Fig. 2). Parameters of the Gaussian bands, into which these spectra were decomposed, are given in Table 1.

Some of these bands can be assigned to specific co-factors according to published data: bands 1 (at 796 nm) and 2 (816 nm) with relative amplitudes of 0.27 and 0.35 as well as 37 and 22 nm FWHM, can be ascribed to H_B and H_A, respectively. This assignment is based on low-temperature absorption data obtained with reduced RCs of *B. viridis* [19]. According to Ref. [19], the absorption maximum of H_B is located at 790 nm at 5 K, whereas H_A was found to peak at 805 and 810 nm at 5 and 110 K, respectively [18,19]. A blue shift of the Q_y band of H upon cooling in comparison to RT is a well-known phenomenon [32]. The narrowest band 4 with maximum at 831 nm (17 nm FWHM) is ascribed to the Q_y transition of the monomeric BChls. This is the most intense band in our decomposition analysis. It is well known that the absorption spectra of both, B_B and B_A, strongly overlap and form an intensive peak at 830 nm at 300 K [21]. Finally, band 6 with a maximum at 960 nm (77 nm FWHM) and relative amplitude of 0.34 corresponds to the P_{y-} component in *B. viridis* RCs [19–21]. The very broad band 3 with an 818 nm maximum (110 nm FWHM) is apparently the superposition of the vibronic subbands of all bacteriochlorin components in the RC. The assignment of the remaining band 5 peaking at 842 nm will be discussed below.

The absorption spectrum of the oxidized RC is shown in Fig. 3 (open circles). From comparison of the respective amplitudes of band 4 (Table 1) it can be seen that the addition of 5 mM ferricyanid caused only partial oxidation (~75%) of P in RCs of *B. viridis*. As in the case of the reduced RC, the absorption spectrum of the oxidized RC was decomposed into 6 Gaussian bands (Fig. 3, thin lines). A closer inspection of the band positions, their amplitudes and FWHM for oxidized and reduced RC preparations shows that the Gaussian parameters of the subbands are altered to different extents: maximum position, amplitude and FWHM of band 1 (H_B) are essentially unaltered (Table 1). The 7% gain in amplitude of this band in oxidized RCs in comparison to the reduced ones does not exceed the decomposition accuracy (cf. Materials and methods). The same holds for the difference in band position, amplitude and FWHM of the bands 1, 2 and 3, assigned to B, H_A and to the superposition of the vibronic subbands, respectively, in the absorption spectra of the oxidized and reduced RCs (Figs. 2, 3 and Table 1). In the experimental spectra (Figs. 2, 3) the observed shift of the B band upon oxidation of P is ~5 nm, a value consistent with previous reports for RCs of *B. viridis* [32,33] and *R. sphaeroides* [12,32–34]. The shift of the position of B to the blue in the oxidized RCs is usually explained as an electrochromic shift caused by P^+ formation [12,23,27,28] or due to absence of coupling with the special pair excitonic states [12]. Obviously, the ~5 nm blue shift of the B band upon P oxidation observed by comparison of the absorption spectra of the reduced and oxidized *B. viridis* RCs is the combined effect of at least two processes: P_{y+} band bleaching and the influence of the electric field of P^+ (electrochromic effect). A contribution of these two processes to the blue shift will be further discussed below.

Let us discuss the origin of band 5 (Table 1) now. Absorption maximum and FWHM of this band for reduced and oxidized RCs are 842 and 23 nm. The relative amplitude of the 842 nm band in the reduced RC is 0.38 and strongly depends on the amount of P^+ in the RC preparation. The amount of oxidized RCs was assessed by comparison of the amplitude of the 960 nm band in control and potassium ferricyanide treated RC preparations. By incubation of the RC preparations with 1 mM potassium ferricyanide for 5 min 50% oxidation of P was achieved. In this preparation the intensity of the 842 nm band was 0.2 (data not shown). Upon oxidation of 75% of the RCs by addition of 5 mM $K_3Fe(CN)_6$ the amplitude of the 842 nm band was decreased to 0.1 (Fig. 3 and Table 1). Finally, essentially full oxidation of P was obtained by the addition of an excess of $K_3Fe(CN)_6$ to the RC preparation, a procedure that results in oxidation of more than 95% of P. In this case the band with the

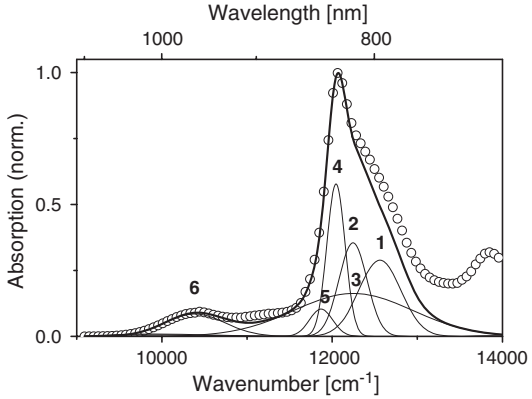

Fig. 3. Room temperature Q_y absorption spectrum of 75% oxidized RCs from *B. viridis* upon addition of 5 mM $K_3Fe(CN)_6$ (circles). Gaussian bands into which the experimental spectrum was decomposed are shown as thin curves. The thick curve represents the envelope of the Gaussian subbands.

Table 1
Parameters obtained by decomposition of the absorption spectra of reduced and oxidized RCs from *B. viridis* into Gaussian bands

№	Peak position [nm/cm^{-1}]		Amplitude [rel. units]		FWHM [nm/cm^{-1}]	
	Reduced RC	Oxidized RC	Reduced RC	Oxidized RC	Reduced RC	Oxidized RC
1	796/12 563	796/12 563	0.27	0.29	37/584	37/584
2	816/12 255	817/12 240	0.35	0.35	22/330	26/390
3	818/12 225	816/12 255	0.16	0.16	110/1651	110/1660
4	831/12 034	830/12 048	0.54	0.58	17/246	17/247
5	842/11 876	842/11 876	0.38	0.10	23/324	23/324
6	960/10 417	962/10 395	0.34	0.09	77/837	77/833

absorption maximum at 842 nm disappeared. The absorption spectrum of fully oxidized samples was decomposed into mere 5 Gaussian bands with maxima at 796, 816, 817, 830 and 962 nm (data not shown). Thus, a synchronous reduction of the amplitudes of the 842 and 960 nm absorption bands upon oxidation of a progressive number of the P was observed. This observation is an important evidence that the band with a maximum at 842 nm in the absorption spectrum of the reduced RC from *B. viridis* is predominantly related to the P → P_{y+} transition at RT.

In the following the band with a maximum at around 830 nm (assigned to B_B and B_A) will be discussed. The decomposition data summarized in Table 1 indicate that the maximum of this band shifts 1 nm to the blue upon oxidation of P. On the other hand, the experimentally observed blue shift is about 5 nm (compare Figs. 2 and 3). If the B band positions determined from decomposition of the absorption spectra of native and oxidized RC are realistic, this would indicate that the electrochromic shift caused by P oxidation is merely ~1 nm in comparison to the shift due to bleaching of the P_{y+} band (~4 nm). This assumption is confirmed by an analysis of the data presented in Fig. 4, where 2nd derivatives of the absorption spectra of reduced and oxidized RCs are shown. A detailed inspection indicates that upon oxidation of P the maximum of the inverted 2nd derivative of the absorption spectrum of the B band blue shifts by mere 10 cm^{-1}. Moreover, the main difference in the 2nd derivative spectra of reduced and oxidized RCs is observed in the region between 840 and 845 nm, i.e. where a band that is ascribed to P_{y+} is located (Fig. 4). Consequently, the shift of the main NIR absorption maximum at approximately 830 nm upon oxidation is mainly caused by the disappearance of the excitonic band P_{y+}. Oxidation of P also leads to a blue shift of 1 nm (from 831 to 830 nm) of the B_B and B_A bands and to a red shift (from 816 to 817 nm) of the H_A band, as summarized in Table 1. The blue shift of the absorption of the monomeric BChls *b* and the red shift of BPheo upon oxidation of the RC is usually explained by an electrochromic effect, caused by the electric charge on P [32,35]. The accurate displacements have not been determined analytically with certainty, yet, due to the fact, that—in spite of a well-known RC structure—the effective dielectric constant (ε) of the medium surrounding P is uncertain. Thus, estimations resulted in a shift of the bands of the monomeric BChls *b* of 13 nm for ε~4, or 5 nm for ε=10 [36,37].

Results obtained with oxidized RCs from *B. viridis* indicate that the blue shift of the composite (integral) absorption band of porphyrins in the region around 830 nm (Fig. 4) is not primarily determined by electrochromic effects—but rather by the disappearance of an absorption component that can be related to P_{y+}.

3.2. Analysis of the absorption spectra of RCs from R. sphaeroides

Normalized RT NIR absorption spectra of reduced (solid line) and oxidized (dotted line) RCs from the BChl *a*-containing purple bacterium *R. sphaeroides* strain 2R are shown in Fig. 5. Three absorption maxima are observed for reduced RCs: at 864 nm (due to P_{y-}), at 760 nm (due to the BPheos) and, one at about 800 nm. It is generally assumed [12,14,20,23,25–28] that the monomeric BChls *a* and P_{y+} absorb in the latter region.

Table 2
Parameters obtained by decomposition of the absorption spectra of reduced and oxidized RCs from *R. sphaeroides* into Gaussian bands

№	Peak position [nm/cm^{-1}]		Amplitude [rel. units]		FWHM [nm/cm^{-1}]	
	Reduced RC	Oxidized RC	Reduced RC	Oxidized RC	Reduced RC	Oxidized RC
1	802/12 468	801/12 477	0.42	0.42	16/248	16/248
2	810/12 347	–	0.26	–	15/233	–
3	797/12 542	797/12 542	0.29	0.29	17/264	17/264
4	864/11 576	859/11 646	0.45	0.05	60/804	46/629
5	789/12 668	789/12 668	0.27	0.40	19/309	20/324
6	812/12 318	811/12 338	0.14	0.12	29/439	21/320
7	758/13 197	759/13 180	0.12	0.15	16/279	17/289
8	767/13 032	771/12 962	0.22	0.22	42/709	46/769
9	748/13 376	748/13 366	0.10	0.10	17/301	16/291
10	736/13 585	739/13 537	0.19	0.15	41/761	42/776

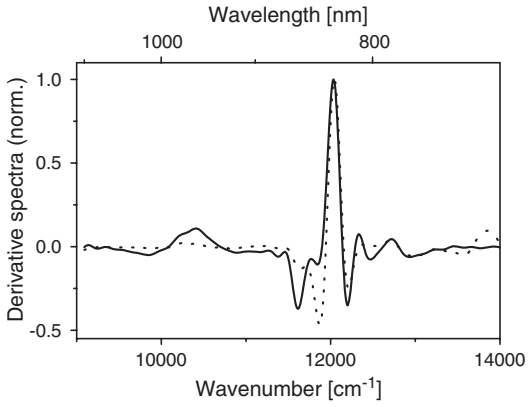

Fig. 4. Inverted normalized 2nd derivatives of the absorption spectra of reduced (solid line) and chemically oxidized (dotted line) RCs of *B. viridis*.

Chemical oxidation of RC preparations with ferricyanide leads to bleaching of the P_{y-} band at 864 nm. Additionally, a red shift of the BPheo absorption band as well as a blue shift (by 3.5 nm) of the 800 nm band are observed. The band shifts observed at approximately 760 and 800 nm upon oxidation of RCs are usually explained by an electrochromic effect [15,17,38] (see also previous section). A contribution of a fading excitonic P_{y+} band to the blue shift of a band at 800 nm can also not be excluded.

Decomposition of the absorption spectra of reduced and oxidized RCs from *R. sphaeroides* into Gaussian bands is shown in Fig. 6a and b. Parameters of the Gaussian bands into which these spectra were decomposed are given in the Table 2. The spectrum of reduced *R. sphaeroides* RCs can be decomposed into 10 Gaussian bands, whereas the spectrum of oxidized RCs can be represented by 9 Gaussian bands (Fig. 6 and Table 2). Derivatives up to the 6th order were used in the decomposition procedure. 2nd, 4th and 6th derivatives of the absorption spectrum of reduced RCs, the model bands as well as the envelope of the combined model bands, respectively, are shown in Fig. 7a, b, c. Evidently, for a satisfactory approximation of all derivatives all resolved model bands are necessary. The bands 1 (at 802 nm) and 2 (at 810 nm) determine

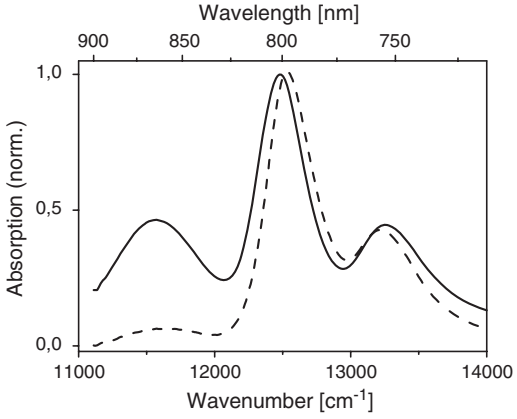

Fig. 5. Q_y absorption spectra of reduced (solid line) and chemically oxidized (dashed line) RCs from the BChl *a* containing purple bacterium *R. sphaeroides* strain 2R at RT.

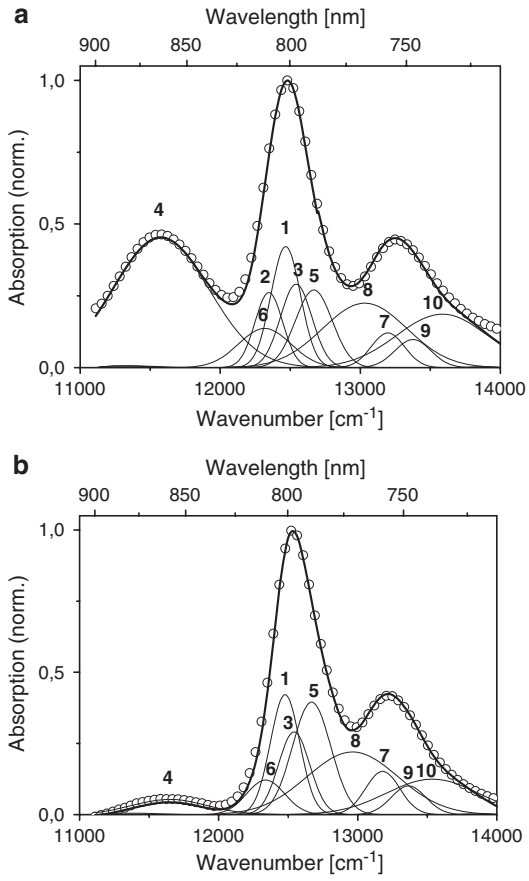

Fig. 6. Decomposition of absorption spectra of reduced (a) and chemically oxidized (b) RCs from *R. sphaeroides* into Gaussian bands. Thin curves show subbands, the thick curve shows their envelope, and circles indicate the original absorption spectra.

the higher order derivatives. Moreover, their parameters—spectral positions, amplitudes and FWHM—can be determined with high accuracy. Band 4 (at 864 nm) barely overlaps with the remaining ones, and its parameters also can also be determined very precisely. More difficult, however, is the estimation of the spectral characteristics of the remaining bands, since these bands do not make decisive contributions to one of the derivatives.

In the BPheo absorption region (725–775 nm) decomposition reveals 4 bands—two broad ones (8 and 10) and two narrow ones (7 and 9). It was shown previously by replacement of BPheo with pheophytin [39] that Q_y bands of H_B and H_A are located at 752 and 762 nm, respectively, at 6 K. Thus, bands 7 and 9 in Table 2 with maxima at 748 and 758 nm can be ascribed to H_B and H_A. A difference of 4 nm in the H_B and H_A band positions as determined here in comparison to previous data [39] may be a result of different RC preparations: whereas wild type bacteria were used in the current study the carotenoidless mutant R-26 was employed in Ref. [39]. Moreover, the differences in the positions of bands 7 and 9 may be a consequence of the accuracy of Gaussian band fitting. Two broad bands (8 and 10) in the $H_{A,B}$ absorption region are vibronic. Apparently, one broad and one narrow band are required to describe the Q_y band (and its derivatives) of each

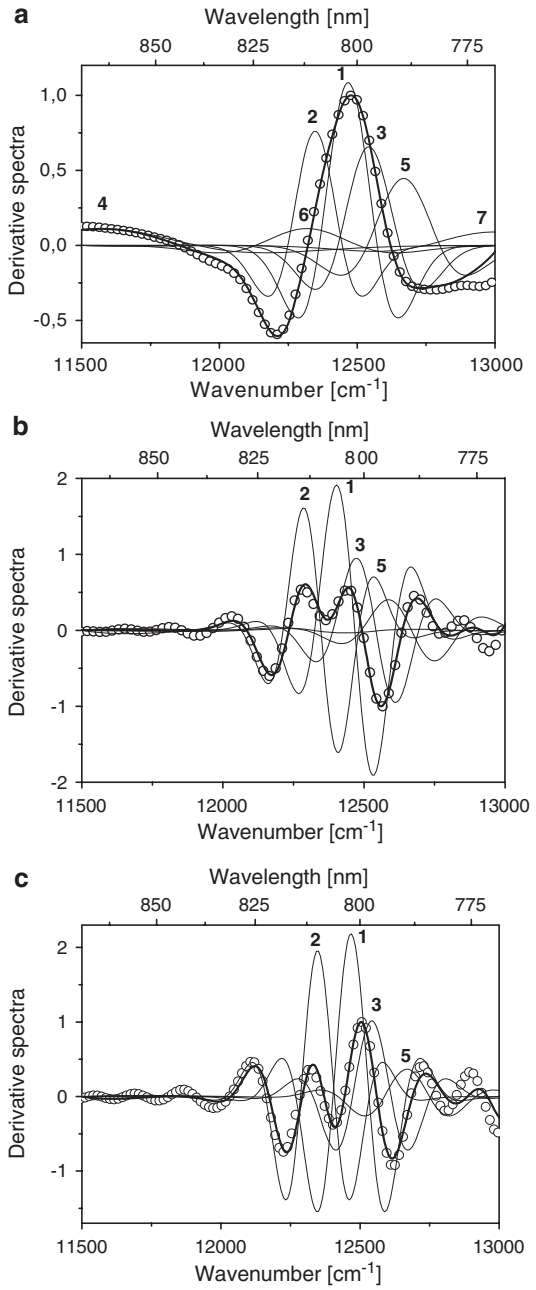

Fig. 7. Derivatives of the spectra of reduced RCs from *R. sphaeroides*. Circles represent the derivatives of the experimental absorption band; thick lines are the derivatives of the envelope of the model bands; thin lines are the derivatives of the Gaussian bands shown in Fig. 5. a) 2nd derivatives; b) 5th derivatives; c) 6th derivatives.

BPheo: the 736 and 748 nm bands for approximation of H_B and the 767 and 758 nm bands to fit the H_A band.

5 Gaussian bands are resolved in the 800 nm region for reduced RCs. For the same region, 4 Gaussian bands are obtained for oxidized RCs. Apparently, a decomposition of the composite (integral) band centered at approximately 800 nm results in more Gaussians than the number of individual pigments in the RC. This is not surprising, since even the Q_y absorption band of a monomeric (B)Chl (in a proteinaqueous environment) has a complex shape due to of the presence of a set of vibronic modes. Examples for theoretical calculations of the shape of the Chl *a* Q_y absorption band in different environments with the aid of the experimentally obtained vibronic frequencies and Frank–Condon factors can be found in Ref. [31]. As shown in Ref. [29], the Q_y band of a monomeric Chl *a* can be approximated by a combination of Gaussians. In this case the prevailing contribution comes from the narrowest band. The remaining model bands have considerably smaller amplitudes and larger widths. Consequently, it is reasonable to assume that the narrowest model bands (3 peaking at 797 nm, 1 with maximum at 802 nm and 2 located at 810 nm) which provide the main contributions to the higher order derivatives of the absorption spectra of both, oxidized and reduced RCs from *R. sphaeroides* are the determinant model bands of three individual absorption bands (two monomeric BChls *a* and P_{y+}). The broad model bands (5 and 6) are probably vibronic structures. These vibronic bands combine contributions from all BChl *a* components of the RC: B_A, B_B, P_{y+}, P_{y-}(the presence of a long "tail" of the P_{y-}band in this region was previously deduced [20]).

Bands 1 (with maximum at 802 nm) and 3 (peaking at 797 nm) in reduced and oxidized RCs are characterized by essentially the same FWHM (16 and 17 nm, respectively) but rather different amplitudes (Fig. 6a and b and Table 2). The maximum of band 1 is very close to the position of the maximum of the original absorption band assigned to B_B [40]. Band 3 apparently can be attributed to B_A. However, in that case the spectral distance between the B_B and B_A bands would be less than estimated previously (125 cm^{-1}), cf. e.g., Ref. [20]. Notably, the position of band 3 as obtained by our decomposition is determined with less accuracy than the position of the band 1. Nevertheless, we believe that Gaussian bands 3 and 1 are related to B_A and B_B, respectively.

Of considerable interest is the origin of band 2 (Table 2). Absorption maximum and FWHM of this band for reduced RCs are 810 and 15 nm, respectively. The relative amplitude of the 810 nm band for the reduced RC is 0.26. Upon oxidation of more than 90% of the RCs by the addition of 1 mM $K_3Fe(CN)_6$, the amplitude of the 810 nm band decreased to near zero (see Table 2). In this case, the absorption spectrum of the oxidized *R. sphaeroides* was decomposed into 9 Gaussian bands, (Fig. 6b). Obviously, band 4 with maximum at 864 nm is related to P_{y-} in *R. sphaeroides* RCs. Moreover, a similar reduction in the amplitudes of the 810 and 864 nm absorption bands upon oxidation of RCs in *R. sphaeroides* was observed. Comparison of the results regarding the 810 nm band with the data in the literature [12,23,25–28] related to the position of the P_{y+} band allows us to conclude that the 810 nm band found in the absorption spectrum of the reduced RC from *R. sphaeroides* can be ascribed to $P \rightarrow P_{y+}$ transition at RT. An estimation of the dipole strengths of the P_{y+} and P_{y-} transitions was conducted on the basis of the decomposition results. The dipole strengths of the bands were calculated according to the procedure given in Ref. [41] from the area under the absorption bands. It was found that the ratio of the dipole strengths of P_{y+} to P_{y-} is close to 1 : 6 — a ratio which is consistent with previous estimates [12,42]. Higher-order derivative analysis also supports our conclusion

regarding the origin of the 810 nm absorption band, see also below.

Since broad bands make only minor contributions to higher order derivatives, comparison of the higher derivative spectra (in which the contributions from broad bands are insignificant) of reduced and oxidized RCs appears to be useful. 2nd and 4th derivative spectra of reduced and oxidized RCs are shown in Fig. 8a and b. The 2nd derivative spectrum indicates that the shift of the maximum of the oxidized RCs is significantly less pronounced as compared to the initial absorption spectrum (see Fig. 5). In the 5th derivative this shift is virtually absent. The corresponding derivatives of the combined model bands obtained for the spectrum of reduced RCs are given, with exception of band 2 (Fig. 8a and b). Apparently, the derivatives of this combination of model bands (without band 2) barely differ from the corresponding derivatives of the absorption spectrum of oxidized RCs. This clearly indicates that the main difference between the set of relatively narrow model bands (contributing dominantly to the higher derivatives) between reduced and oxidized RCs is entirely due to band 2. The latter observation confirms the above conclusion about association of this band with the P_{y+} of the BChl *a* dimer. Additionally, it

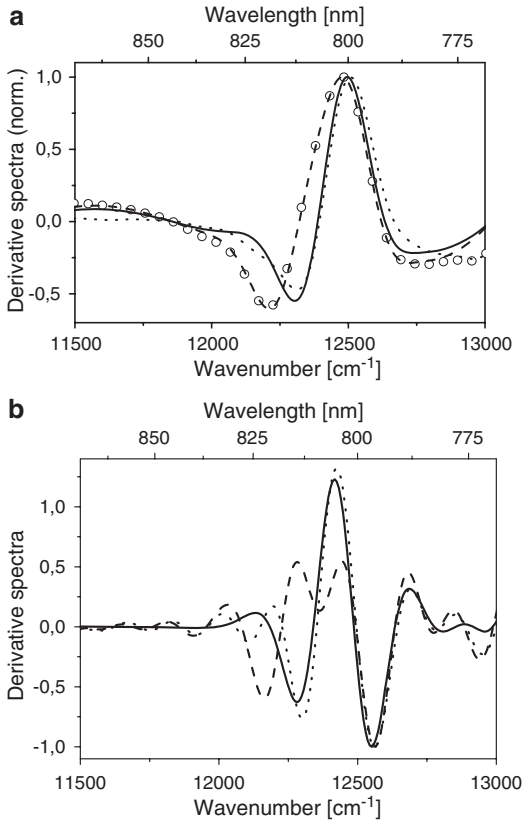

Fig. 8. 2nd (a) and 5th (b) derivatives of absorption spectra of RCs from *R. sphaeroides*. Circles represent the derivatives of the spectrum of reduced RCs. Dotted lines are the derivatives of the absorption spectrum of oxidized RCs. Dashed curves represent the derivatives of the envelope of the subbands into which the absorption spectrum of the reduced RCs was decomposed (Fig 5a, thick line). Additionally, the derivatives of the envelope of the model bands for the absorption spectrum of reduced RCs with exception of band 2 are shown by the solid line.

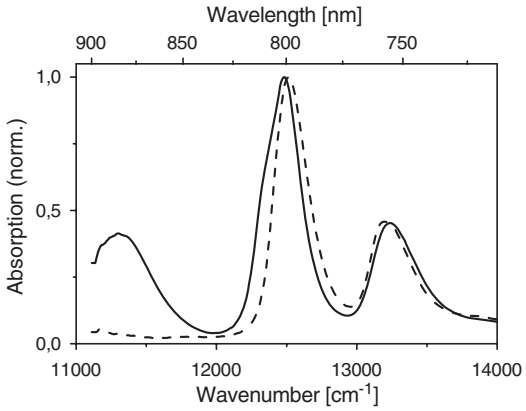

Fig. 9. Low-temperature (77 K) absorption spectra of reduced (solid line) and chemically oxidized (dashed line) RCs of *R. sphaeroides*.

follows that the blue shift of integral band at approximately 800 nm observed upon oxidation of RCs is caused primarily by the disappearance of the P_{y+} exciton component of the special pair. The shift of the absorption band of monomeric BChls *a* upon oxidation of RCs is considerably less pronounced (about 10 cm^{-1}).

Additional information for the study of the substructure of complex optical spectra can be obtained from low-temperature measurements. 77 K absorption spectra of our RC preparations in the reduced and oxidized states are represented in Fig. 9. 2nd derivatives of these spectra are given in Fig. 10. A shoulder at 811 nm is clearly observed in the absorption spectrum of reduced RCs. The inverted 2nd derivative of the absorption spectrum of reduced RCs shows a pronounced maximum in this (811 nm) region. This particular feature disappears upon oxidation of the RC and, consequently, can be attributed to the P_{y+} band. This observation indicates that the maximum of the P_{y+} band is less temperature-dependent than previously suggested [20]. Accordingly it was assumed that P_{y+} peaks at 814 nm (at 298 K) or at 810 nm (at 77 K) [20]. Notably, the shift of the integral band at approximately 800 nm into the short-wavelength region upon oxidation of RCs at 77 K (Fig. 9) is less pronounced (2 nm) than at 298 K (3.5 nm, compare Fig. 5). The latter observation may be explained by a significant narrowing of the absorption bands of

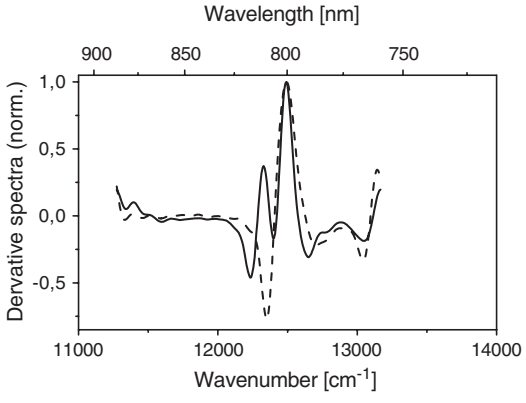

Fig. 10. 2nd derivatives of the 77 K absorption spectra of reduced (solid line) and chemically oxidized (dashed line) RCs of *R. sphaeroides*.

the individual RC components at 77 K. Consequently, the disappearance of the P_{y+} band in oxidized RCs (providing the most pronounced contribution to this shift) must lead to a less pronounced effect at low temperatures.

Thus, as suggested by the results presented here, the method of analyzing multicomponent spectral bands in absorption spectra of purple bacterial RCs by higher-order derivative spectroscopy provides useful information, in particular for the identification of individual components of the complex integral absorption band in the region around 800 nm. The data can be used, e.g., for a precise estimation of the magnitude of electrochromic effects upon charge separation in RCs, as well as for the calculations of interaction energies in the special pair upon changing the ambient conditions (temperature, chemical environment, etc.).

The results obtained in the present study indicate that the upper exciton level P_{y+} of the photo-active BChl *a* dimer in RCs of *R. sphaeroides* has an absorption maximum of 810 nm. The blue shift of a complex integral band at approximately 800 nm as observed upon oxidation of the RCs is caused primarily by bleaching of the P_{y+} excitonic component, rather than by an electrochromic shift of the absorption band(s) of the monomeric BChls *a*, B_A and B_B. Similarly, the disappearance of a band peaking at 842 nm in RC preparations from *B. viridis* upon oxidation indicates that this band has also to be assigned to P_{y+}. A blue shift of an absorption band peaking at approximately 830 nm as observed upon oxidation of RCs of *B. viridis* is caused essentially by the disappearance of P_{y+}, and not by an electrochromic shift of the absorption bands of the monomeric BChls *b*.

4. Conclusions

The knowledge of the exact position of the P_{y+} energy level has significant implications for the mechanisms of ultrafast EET and charge separation in photosynthetic RCs. Indeed, the overlap between the fluorescence spectrum of monomeric BChl *a* molecules, first observed for functional RCs of *R. sphaeroides* [43], and the absorption spectrum of the terminal excitation energy acceptor is very low. Obviously, an intermediate energy level between the levels of the donors (H, B) and the acceptor (P) must exist to facilitate effective EET. Apparently, P_{y+} serves as this energetic intermediate. Our investigations indicate that P_{y+} peaks at 810 and 842 nm for RCs of *R. sphaeroides* and *B. viridis*, respectively. The maximum position of the $P \rightarrow P_{y+}$ absorption band determined in this study for RCs of *R. sphaeroides* (810 nm at 296 K) is very close to values determined previously (811 nm at 4.2 K; 813 nm at 77 K and 805–810 nm at 8 K [23,27,28]). It differs, however, from values (825 nm at 218 K; 814 or 815 nm at 77 K) as presented in Refs. [12,25,26]. The overlap between BChl *a* emission with ground state absorption of P_+ is a significant factor influencing the rate of BChl *a* $\rightarrow P_{y+}$ EET [44]. Based on time-resolved BChl *a* fluorescence spectra [43] and calculated absorption properties of P_{y+}, as depicted in Fig 6a (curve 6) and Table 2 it is deduced that the BChl *a* $\rightarrow P_{y+}$ EET rate can achieve almost maximal values. Owing to the precision of our Q_y band decomposition the peak position of the P_{y+} band reported for the *R. sphaeroides* RC is believed to be highly accurate. Very recently [45] we have studied the spectral and temporal dynamics of the transient states in the 780–830 nm spectral region by transient absorption spectroscopy with 70 fs time resolution using similar *R. sphaeroides* RC preparations as in the current communication. It was found that P_{y+} is located at 809 nm for RCs of *R. sphaeroides* [45], which is very close to the spectral position (810 nm) determined in this study. The upper exciton state P_{y+} of P in *B. viridis* was found to be located at 842 nm. This value is close to the calculated one (850 nm) [20] but significantly differs from previous results obtained by theoretical analyses of absorption and CD spectra (811 nm at RT) [11] as well as dichroic transient absorption spectroscopy (855 nm) [21]. Time-resolved fluorescence spectra should be very useful for the calculation of that particular P_{y+} position for which the maximum BChl *b* $\rightarrow P_{y+}$ EET rate would be achieved in *B. viridis* RCs. The position of P_{y+} in *B. viridis* RCs as determined in this study by higher order derivative spectroscopy is a new—independent—result useful for understanding EET mechanism (s) in RCs of BChl *b*-containing purple bacteria. To further substantiate our results time-resolved investigations of the spectral dynamics in *B. viridis* RCs are currently underway in our labs.

Another interesting result of the current study pertains to the origin of the 4–5 nm blue shift of the B band in *R. sphaeroides* and *B. viridis* RCs upon dark oxidation of P. This shift is generally explained by an electrochromic effect of the positive charge created on P upon oxidation [14–16,25]. Our results indicate that blue shift of the B band in oxidized *R. sphaeroides* and *B. viridis* RCs is mainly caused by the disappearence of the P_{y+} excitonic band.

It is important to note that a more significant blue shift of the B band is indeed observed when RC samples are in the P^+BH^-Q state [7,12–14,20,21,33]. This blue shift of B is usually also explained as an electrochromic effect. We suggest that the physical origin of the blue shift for RCs in the P^+BHQ and P^+BH^-Q states is different: In the P^+BHQ state the electric field of the point positive charge influences the B molecules. In this case the electrochromic effect is rather weak and a 4 nm shift is the result of P_{y+} band bleaching. In contrast, when an electron is transferred to H, the monomeric B molecules are located in the electrical field of the dipole $P^{+\cdot}-H^{-\cdot}$. It is suggested that—in the latter case—a pronounced blue shift (up to 20 nm) of the photoinduced transient absorption spectrum is caused essentially by an electrochromic effect. Upon electron transfer from H^- to Q_A, the B molecules are assumed to be subjected to an electric field of the $P^{+\cdot}Q_A^{-\cdot}$ dipole ($P^+BHQ_A^-$ state of RC). The influence of the electric field on the B molecules in the configuration $P^+BHQ_A^-$ is less pronounced than that in the configuration $P^+BH^-Q_A$. Consequently, the photo-induced blue shift of the B band in the former state (~10 nm) is two times less than in the latter case (~20 nm). This supports our proposal that the electrochromic shift of the B band is evoked by the electric field of the dipoles $P^{+\cdot}Q_A^{-\cdot}$ or $P^{+\cdot}Q_A^{-\cdot}$. In the dark-oxidized RC (state P^+BHQ_A) the 4–5 nm blue shift is essentially the result of P_{y+} bleaching.

Acknowledgements

Partial financial support is gratefully acknowledged: Russian Foundation for Basic Research (Projects Nos. 04-04-49486, 05-04-48606 and 06-04-49072), and MNP of MGU, as well as DFG (SFB 429, TP A2).

References

[1] J. Deisenhofer, O. Epp, K. Miki, R. Huber, H. Michel, X-ray structure-analysis of a membrane–protein complex—electron-density map at 3 Å resolution and model of the chromophores of the photosynthetic reaction center from *Rhodopseudomonas viridis*, J. Mol. Biol. 180 (1984) 385–398.

[2] G. Feher, J.P. Allen, M.Y. Okamura, D.C. Rees, Structure and function of bacterial photosynthetic reaction centers, Nature 339 (1989) 111–116.

[3] U. Ermler, G. Fritzsch, S.K. Buchanan, H. Michel, Structure of the photosynthetic reaction-center from *Rhodobacter sphaeroides* at 2.65 Ångström resolution—cofactors and protein–cofactor interactions, Structure 2 (1994) 925–936.

[4] C.R.D. Lancaster, U. Ermler, H. Michel, The structures of photosynthetic reaction centers from purple bacteria as revealed by X-ray crystallography, in: R.E. Blankenship, M.T. Madigan, C.E. Bauer (Eds.), Anoxygenic Photosynthetic Bacteria, Kluwer, Dordrecht, Netherlands, 1995, pp. 503–526.

[5] C. Kirmaier, D. Holten, W.W. Parson, Temperature and detection-wavelength dependence of the picosecond electron-transfer kinetics measured in *Rhodopseudomonas sphaeroides* reaction centers. Resolution of new spectral and kinetic components in the primary charge-separation process, Biochim. Biophys. Acta 810 (1985) 33–48.

[6] V.A. Shuvalov, L.N.M. Dyusens, Primary electron transfer reactions in modified reaction centers from *Rhodopseudomonas sphaeroides*, Proc. Natl. Acad. Sci. U. S. A. 83 (1986) 1690–1694.

[7] A.R. Holzwarth, M.G. Müller, Energetics and kinetics of radical pairs in reaction centers from *Rhodobacter sphaeroides*. A femtosecond transient absorption study, Biochemistry 35 (1996) 11820–11831.

[8] W. Zinth, J. Wachtveitl, The first picoseconds in bacterial photosynthesis —ultrafast electron transfer for the efficient conversion of light energy, ChemPhysChem 6 (2005) 871–880.

[9] J. Eccles, B. Honig, Charged amino acids as spectroscopic determinants for chlorophyll in vivo, Proc. Natl. Acad. Sci. U. S. A. 80 (1983) 4959–4962.

[10] A. Scherz, W. Parson, Exciton interactions in dimers of bacteriochlorophyll and related molecules, Biochim. Biophys. Acta 766 (1984) 666–678.

[11] E. Knapp, S. Fischer, W. Zinth, M. Sander, W. Kaiser, J. Deisenhofer, H. Michel, Analysis of optical spectra from single crystals of *Rhodopseudomonas viridis* reaction centers, Proc. Natl. Acad. Sci. U. S. A. 82 (1985) 8463–8467.

[12] D.C. Arnett, C.C. Moser, P.L. Dutton, N.F. Scherer, The first events in photosynthesis: electronic coupling and energy transfer dynamics in the photosynthetic reaction center from *Rhodobacter sphaeroides*, J. Phys. Chem., B 103 (1999) 2014–2032.

[13] V.A. Shuvalov, A.G. Yakovlev, Coupling of nuclear wavepacket motion and charge separation in bacterial reaction centers, FEBS Lett. 540 (2003) 26–34.

[14] N.W. Woodbury, J.P. Allen, The pathway, kinetics and thermodynamics of electron transfer in wild type and mutant reaction centers of purple nonsulphur bacteria, in: R.E. Blankenship, M.T. Madigan, C.E. Bauer (Eds.), Anoxygenic Photosynthetic Bacteria, Kluwer Acad. Publ., Dordrecht, Netherlands, 1995, pp. 528–557.

[15] W.W. Parson, Reaction centers, in: H. Scheer (Ed.), Chlorophylls, CRC Press, Boca Raton, 1991, pp. 1153–1180.

[16] J. Breton, Orientation of the chromophores in the reaction center of *Rhodopseudomonas viridis*. Comparison of low-temperature linear dichroism spectra with a model derived from X-ray crystallography, Biochim. Biophys. Acta 810 (1985) 235–245.

[17] W.W. Parson, The bacterial reaction center, in: J. Amesz (Ed.), Photosynthesis, Elsevier, Amsterdam, 1988, pp. 43–61.

[18] D.M. Tiede, E. Kellogg, J. Breton, Conformational changes following reduction of the bacteriopheophytin electron acceptor in reaction centers of *Rhodopseudomonas viridis*, Biochim. Biophys. Acta 892 (1987) 294–302.

[19] J. Eccles, B. Honig, K. Schulten, Spectroscopic determinants in the reaction center of *Rhodopseudomonas viridis*, Biophys. J. 53 (1988) 137–144.

[20] X.J. Jordanides, G.D. Scholes, G.R. Fleming, The mechanism of energy transfer in the bacterial photosynthetic reaction center, J. Phys. Chem., B 105 (2001) 1652–1669.

[21] P.O.J. Scherer, S.F. Fischer, C.R.D. Lancaster, G. Fritzsch, S. Schmidt, T. Arlt, K. Dressler, W. Zinth, Time-resolved spectroscopy of the excited electron state of reaction centers of *Rhodopseudomonas viridis*, Chem. Phys. Lett. 223 (1994) 110–115.

[22] J.C. Williams, R.G. Alden, H.A. Murchison, J.M. Peloquin, N.W. Woodbury, J.P. Allen, Effects of mutation near the bacteriochlorophylls in reaction centers from *Rhodobacter sphaeroides*, Biochemistry 31 (1992) 11029–11037.

[23] G. Hartwich, H. Scheer, V. Aust, A. Angerhofer, Absorption and ADMR studies on bacterial photosynthetic reaction centres with modified pigments, Biochim. Biophys. Acta 1230 (1995) 97–113.

[24] H. Scheer, G. Hartwich, Bacterial reaction centers with modified tetrapyrrole chromophores, in: R. Blankenship, M.T. Madigan, C.E. Bauer (Eds.), Anoxygenic Photosynthetic Bacteria, Kluwer, Dordrecht, 1995, pp. 649–663.

[25] J. Breton, Low temperature linear dichroism study of the orientation of the pigments in reduced and oxidized reaction centers of the photosynthetic bacteria *Rps. viridis* and *Rb. sphaeroides*, in: J. Breton, A. Vermeglio (Eds.), The Photosynthetic Bacterial Reaction Centers: Structure and Dynamics, Plenum Press, New York, 1988, pp. 59–69.

[26] L.M.P. Beekman, I.H.M. van Stokkum, R. Monshouwer, A.J. Rijnders, P. McGlynn, R.W. Visschers, M.R. Jones, R. van Grondelle, Primary electron transfer in membrane-bound reaction centers with mutations at the M210 position, J. Phys. Chem. 100 (1996) 7256–7268.

[27] S.G. Johnson, D. Tang, R. Jankowiak, J.M. Hayes, G.J. Small, D.M. Tiede, Structure and marker mode of the primary electron donor state absorption of photosynthetic bacteria: hole-burned spectra, J. Phys. Chem. 93 (1989) 5953–5957.

[28] S.R. Meech, A.J. Hoff, D.A. Wiersma, Role of charge-transfer states in bacterial photosynthesis, Proc. Natl. Acad. Sci. U. S. A. 83 (1986) 9464–9468.

[29] I.K. Mikhailyuk, H. Lokstein, A.P. Razjivin, A method of spectral subband decomposition by simultaneous fitting the initial spectrum and a set of its derivatives, J. Biochem. Biophys. Methods 63 (2005) 10–23.

[30] N.I. Zakharova, I.Yu. Churbanova, Methods of isolation of reaction center preparations from photosynthetic purple bacteria, Biochemistry (Moscow) 65 (2000) 149–159.

[31] G. Zucchelli, R.C. Jennings, F.M. Garlaschi, G. Cinque, R. Bassi, O. Cremonesi, The calculated in vitro and in vivo chlorophyll a absorption bandshape, Biophys. J. 82 (2002) 378–390.

[32] C. Kirmaier, D. Holten, Primary photochemistry of reaction centers from the photosynthetic purple bacteria, Photosynth. Res. 13 (1987) 225–260.

[33] T.L. Netzel, P.M. Rentzepis, D.M. Tiede, R.C. Prince, P.L. Dutton, Effect of reduction of the reaction center intermediate upon the picosecond oxidation reaction of the bacteriochlorophyll dimer in *Chromatium vinosum* and *Rhodopseudomonas viridis*, Biochim. Biophys. Acta 460 (1977) 467–479.

[34] J.A. Jackson, S. Lin, A.K.W. Taguchi, J.C. Williams, J.P. Allen, N.W. Woodbury, Energy transfer in *Rhodobacter sphaeroides* reaction centers with the initial electron donor oxidized or missing, J. Phys. Chem. 101 (1997) 5447–5754.

[35] W.W. Parson, Photosynthetic bacterial reaction centers: interactions among the bacteriochlorophylls and bacteriopheophytins, Ann. Rev. Biophys. Bioeng. 11 (1982) 57–80.

[36] B. Honig, W. Hubbel, R. Flewelling, Electrostatic interactions in membranes and proteins, Annu. Rev. Biophys. Biophys. Chem. 15 (1986) 163–193.

[37] M. Gilson, B. Honig, The dielectric constant of a folded protein, Biopolymers 25 (1986) 2097–2119.
[38] R.K. Clayton, Photosynthesis. Physical Mechanisms and Chemical Patterns, Cambridge University Press, Cambridge, 1981.
[39] E.M. Franken, A.Ya. Shkuropatov, C. Franke, S. Neerken, P. Gast, V.A. Shuvalov, A.J. Hoff, T.J. Aartsma, Reaction centers of *Rhodobacter sphaeroides* R-26 with selective replacement of bacteriopheophytin by pheophytin *a*: 1. Characterization of steady-state absorbance and circular dichroism, and of the $P^{+}Q_{A}^{-}$ state, Biochim. Biophys. Acta 1319 (1997) 242–250.
[40] A. de Winter, S.G. Boxer, The mechanism of triplet energy transfer from the special pair to the carotenoid in bacterial photosynthetic reaction centers, J. Phys. Chem., B 103 (1999) 8786–8789.
[41] S. Mukamel, Principles of Nonlinear Optical Spectroscopy, Oxford University Press, New York, 1995, 523 pp.
[42] J.R.S. Reddy, S.V. Kolaczkowski, G.J. Small, Nonphotochemical hole-burning of the reaction center of *Rhodopseudomonas viridis*, J. Phys. Chem. 97 (1995) 6934–6940.
[43] B.A. King, T.B. McAnaney, A. de Winter, S.G. Boxer, Excited state energy transfer pathways in photosynthetic reaction centers: 3. Ultrafast emission from the monomeric bacteriochlorophylls, J. Phys. Chem. 104 (2000) 8895–8902.
[44] J.M. Jean, C.K. Chan, G.R. Fleming, Electronic energy transfer in photosynthetic reaction centers, Isr. J. Chem. 28 (1988) 169–175.
[45] V.V. Gorokhov, V.Z. Paschenko, O.M. Sarkisov, A.B. Rubin, Spectral and temporal dynamics of transient processes in *Rb. sphaeroides* RCs in the 780–830 nm spectral domain, Doklady RAS 406 (2006) 1–4.